Connecting blazars with ultra high energy cosmic rays and astrophysical neutrinos

Elisa Resconi,[1] Stefan Coenders,[1] Paolo Padovani,[2,3] Paolo Giommi,[4,5] and Lorenzo Caccianiga[1]

[1] *Technische Universität München, Physik-Department, James-Frank-Str. 1, D-85748 Garching bei München, Germany*
[2] *European Southern Observatory, Karl-Schwarzschild-Str. 2, D-85748 Garching bei München, Germany*
[3] *Associated to INAF – Osservatorio Astronomico di Roma, via Frascati 33, I-00040 Monteporzio Catone, Italy*
[4] *Italian Space Agency, ASI, via del Politecnico s.n.c., I-00133 Roma Italy*
[5] *ICRANet-Rio, CBPF, Rua Dr. Xavier Sigaud 150, 22290-180 Rio de Janeiro, Brazil*

(Dated: July 29, 2016)

We present evidence of a direct connection between high energy γ-ray emitting blazars, very high energy neutrinos, and ultra high energy cosmic rays. We first identify potential hadronic sources by selecting γ-ray emitters, that are in spatial coincidence with neutrinos detected by IceCube. These are then correlated with ultra high energy cosmic rays from the Pierre Auger Observatory and the Telescope Array scanning in γ-ray flux F_γ and angular separation between sources and cosmic rays θ. A maximal excess of 80 cosmic rays (41.9 expected) is observed for the second catalog of hard *Fermi*-LAT (2FHL) objects with $F_\gamma\,(>50\,\mathrm{GeV}) \geq 1.8\times10^{-11}\,\mathrm{ph\,cm^{-2}\,s^{-1}}$ and $\theta \leq 10^\circ$. The probability for this to happen is 1.6×10^{-5}, which translates to 5.5×10^{-4} (3.26σ) after compensation for trials. No excess of cosmic rays is instead observed for γ-ray blazars *not* in spatial connection with IceCube neutrinos. A likelihood ratio test favors a connection between blazars and cosmic rays via neutrinos with a p-value of 4.1×10^{-4} (3.35σ). The γ-ray sources that make up the excess are blazars of the high synchrotron peak type, which we propose here as ultra high energy cosmic ray and neutrino emitters.

arXiv:1611.06022v1 [astro-ph.HE] 18 Nov 2016

Introduction.– Blazars are Active Galactic Nuclei (AGN) hosting a jet oriented at a small angle with respect to the line of sight with highly relativistic particles moving in a magnetic field and emitting non-thermal radiation [1]. They are among the most luminous and most energetic sources in the Universe. The spectral energy distributions (SEDs) of blazars are composed of two broad humps, a low energy and a high energy one. Based on the rest-frame value of the frequency of the peak of the low energy hump (synchrotron peak, ν_S) blazars of the BL Lac type [2] are called high energy peaked (HBLs) when $\nu_S > 10^{15}$ Hz ($>4\,\mathrm{eV}$). HBLs are the rarest types of blazars, making up $\approx 10\%$ of BL Lacs [3], being at the same time very powerful γ-ray emitters. The idea that blazars of various types could be sources of ultrahigh energy cosmic rays (UHECRs) and, related to that, of high energy neutrinos, has been discussed in e.g. [4, 5] and has since then been explored in a number of studies (see e.g. [6–11]). We perform here detailed statistical studies to test a blazar connection with UHECRs going through high energy neutrinos used as "intermediaries" (see [12] for an extensive review of how cosmic rays are accelerated up to $10^{19}-10^{20}$ eV).

The Pierre Auger Observatory [13, 14] and the Telescope Array (TA) [15] have collected together more than 300 UHECRs with $E \geq 52\times10^{18}\,\mathrm{eV}$ over the entire sky. The former has detected 231 such events covering mostly the southern hemisphere and the latter 72 events above 57×10^{18} eV covering mostly the northern sky. Despite a series of studies on the UHECR arrival direction distributions [16, 17], no counterparts have yet been determined. The strongest deviations from isotropy (post-trial p-values $\sim 1.3-1.4\%$) have been obtained for $E \geq 58\times10^{18}$ eV in connection with Swift AGN closer than 130 Mpc and more luminous than 10^{44} erg $\mathrm{s^{-1}}$, and around the direction of Cen A (at angular separations $\sim 18^\circ$ and $\sim 15^\circ$ respectively) [16]. The distribution of UHECRs does not present statistically significant small scale structures. However, two "hot" regions ($2-3\sigma$ deviations) of about 20° in the cosmic ray sky have been reported (see Fig. 1 left and [16, 18]) but their interpretation is not yet clear.

The IceCube South Pole Neutrino Observatory has recently discovered high energy astrophysical neutrinos and has reported a sample of 54 events collected over a period of four years and with a deposited energy up to 2 PeV [19–21]. These events are coming from the entire sky and make up what we define as the Isotropic Neutrino Emission (IνE). They consist of neutrinos of all flavors, which interact inside the instrumented volume (starting events), the majority of which are shower-like [22]. The complementary sample of through-going charged current ν_μ from the northern sky has also been studied over a period of four years [23] showing that their spectrum is inconsistent with the hypothesis of purely terrestrial origin at the 4.3σ level. Few weeks after submission of this manuscript, the IceCube Collaboration has published more through going tracks [24], not yet included here. The track-like events confirm the general picture of the IνE although their energy spectrum $\mathrm{E}^{-\gamma}$ is harder ($\gamma = 1.91\pm0.20$) with respect to the all sky one obtained from the starting event sample ($\gamma = 2.58\pm0.25$), suggesting a mixed origin of the signal observed by IceCube. Many diverse hypothesis for the

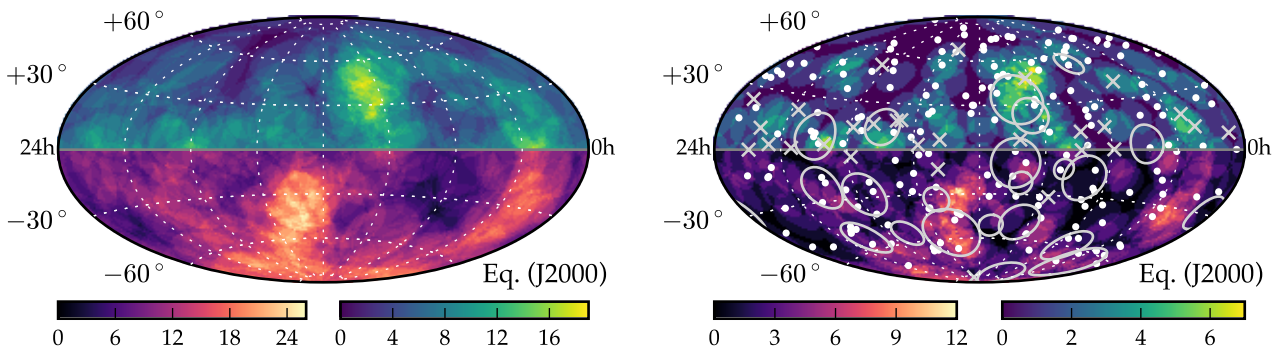

FIG. 1. Sky maps in equatorial coordinates: (left) Auger and TA data as from [16, 18] with uncertainty areas of 20°, roughly the size of the two hot spots found by the collaborations. The color scale indicates the number of events overlapping within the 20° areas; (right) Auger and TA data with uncertainty areas of 10° as obtained from our test with overlaid neutrinos contributing to the test (crosses are track-like events, circles are shower-like events with associated median angular error). White dots indicate the 2FHL (HBL + unclassified sample) as described in the text.

astrophysical counterparts of the IνE have been put forward (see, e.g. [25–32]) but none has so far been statistically supported by the observational data.

In [33] the authors have correlated the second catalog of hard *Fermi*-LAT sources (2FHL) ($E > 50$ GeV, 360 sources of various types, mainly blazars) [34] (and other two catalogs), with the publicly available high energy neutrino sample detected by IceCube [20, 21, 35, 36] (including only events with energy and median angular error ≥ 60 TeV and $\leq 20°$ respectively). The p-value scanning over $F_\gamma\,(> 50\,\mathrm{GeV})$ was 0.4%. We have now also evaluated the impact of the trials, which results in a global p-value of 1.4% (2.2σ). This applies only to HBL blazars and appears to be strongly dependent on γ-ray flux.

In [37], the three collaborations IceCube, Auger, and TA jointly reported about correlation tests between very high energy neutrinos and the same sample of UHECRs used in this paper. All the studies were compatible with the null hypothesis of no correlation although two interesting excesses were observed when considering IceCube shower-like events: a post-trial p-value of 0.05% for an angular scale of 22° provided by the comparison to a randomized UHECR sky, and a p-value of 0.85% obtained by scrambling the neutrinos, thus preserving the existing anisotropies observed in the arrival directions of the UHECRs. As also discussed in [37], the first result (UHECR randomization), is affected by the presence of anisotropies (hot spots) in the UHECR sky (see Fig. 1, left).

Statistical Analysis.– Motivated by the hints mentioned above on (1) an HBL origin of some of the IceCube neutrinos [33], and (2) a common origin of neutrinos and UHECRs [37], we have developed a two-step analysis to investigate the connection between blazars and UHECRs.

Step 1: γ-ray sources to neutrinos (γ - ν).– The neutrinos are implied here as UHECRs' "intermediaries" in order to help single out the best candidate lepto-hadronic accelerators [38] from γ-ray catalogs and hence the most probable cosmic ray sources. We have used all the high energy catalogs presently available including the 2FHL, the 2WHSP [39], and the 3LAC [40], as detailed in [33] and Tab. I, focusing on HBL blazars [41]. The neutrino list is composed of the 51 events (30 starting and 21 tracks) selected by [33]. No further catalog has been tested and all the tests performed on the data are reported here not to hide any trial or relevant information. Although the UHECR horizon is limited by the energy losses caused by the interactions of UHECRs with photons of the Cosmic Microwave Background (CMB), the so-called GZK (Greisen-Zatsepin-Kuzmin) effect [42, 43], we do not apply a-priori cuts on the distance of the cataloged sources. The reason is that a large number of BL Lacs has no measured redshift due to the lack of emission lines in their optical spectra. Moreover, it is difficult to quote a UHECR horizon a priori. Instead of scanning in redshift z as done in other tests [16, 17], we use all sources regardless of their redshift. As done in [33], we have selected γ-ray sources in spatial coincidence with the neutrinos (i.e. within the median angular errors). The selection is done partitioning the flux of the cataloged sources (F_γ) (or alternatively the "figure of merit" (FoM) introduced in the 2WHSP) [44]. With respect to [33], we have here extended the coverage of the sky for 2FHL to the Galactic plane to allow the realization of neutrino scrambled maps as background cases.

Step 2: source candidates to UHECRs (ν - CR).– In a second step, the neutrino selected γ-ray sources at various F_γ (or FoM) are cross correlated with the UHECRs. The correlation is also done as a function of the angular separation θ between the source and the re-

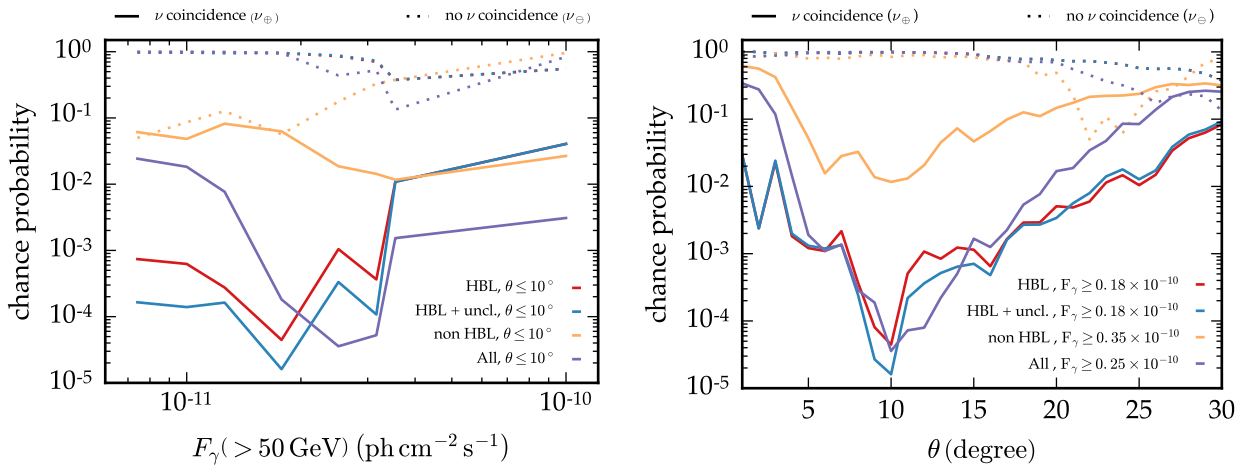
ν coincidence (ν⊕)
no ν coincidence (ν⊖)
chance probability
HBL, θ ≤ 10°
HBL + uncl., θ ≤ 10°
non HBL, θ ≤ 10°
All, θ ≤ 10°
Fγ(> 50 GeV) (ph cm−2 s−1)
HBL , Fγ ≥ 0.18 × 10−10
HBL + uncl. , Fγ ≥ 0.18 × 10−10
non HBL , Fγ ≥ 0.35 × 10−10
All , Fγ ≥ 0.25 × 10−10
θ (degree)

FIG. 2. Result of the statistical test: (left panel) chance probability versus flux F_γ for the 2FHL at a fixed angular distance θ. The probabilities refer to objects having F_γ larger than the value on the x-axis. The angular distance is chosen at the minimum observed in the scan versus angle (right panel). Solid lines show the results for the correlation of UHECRs with γ-rays in coincidence with neutrinos, dashed lines without neutrino coincidence.

constructed incoming direction of the UHECRs over the $1^\circ - 30^\circ$ range in steps of 1°. We quantify the strength of the correlation by counting the number of UHECR events that have *at least* one neutrino selected γ-ray source with F_γ at distance smaller than the angular distance θ and compare this to random trials. This is done by randomizing the right ascension of the neutrino events and repeating the statistical analysis mentioned above. This method ensures that the aforementioned anisotropies in the UHECRs are conserved and do not artificially contribute to the significance of the result, preserving at the same time the IceCube declinations, which are known to be not uniformly distributed. Moreover, for neutrino cascades with large median angular uncertainty, we randomly swap the errors assigned, whereas for track-like events the quoted uncertainty is 0.4° for all events. The p-values are calculated based on random trials. The final result is corrected for trials due to the scanning in F_γ/FoM and θ to search for the largest UHECR excess over the random expectation.

Likelihood ratio test.– A likelihood ratio test is performed to compare the degree of correlation between UHECRs and sources which are not in spatial coincidence with neutrinos (null model $\nu_\ominus$) to the one between UHECRs and sources in spatial coincidence with neutrinos (alternative model $\nu_\oplus$). For both hypotheses $\nu_{\ominus/\oplus}$, F_γ and θ are chosen separately to yield the largest correlation for each hypothesis. The ratio of the models defines the test statistics

$$\Lambda = \frac{\mathcal{P}\left(\gamma - \nu_\ominus - CR; F_{\gamma,\ominus}, \theta_\ominus\right)}{\mathcal{P}\left(\gamma - \nu_\oplus - CR; F_{\gamma,\oplus}, \theta_\oplus\right)}, \qquad (1)$$

where $\mathcal{P}$ is the p-value as defined in the two-step statistical test in the previous section. Large values of Λ indicate preference for a positive correlation of γ-rays with neutrinos and UHECRs. We estimate the significance of this test by comparing data to trials with randomized neutrinos; the p-value is then defined as the chance probability that trials produce a test statistics Λ that is larger than, or equal to that observed.

Results.– We find an excess of UHECRs associated with γ-ray emitting blazars of the HBL type once the sources are spatially pre-selected using the high energy neutrinos detected by IceCube (see Fig. 2 solid lines and Tab. I). The best/minimal p-value is obtained for the 2FHL (HBLs + unclassified sample) with $F_\gamma\,(>50\,\mathrm{GeV}) \geq 1.8\times10^{-11}\,\mathrm{ph\,cm^{-2}\,s^{-1}}$ and $\theta = 10^\circ$. This sample includes all HBLs plus all sources with $2^\circ < |b_{\mathrm{II}}| < 10^\circ$, which are still unclassified in the catalog. By excluding the Galactic plane, in fact, there is a high chance that these sources are unrecognized blazars lying in a region of the sky where the density of stellar sources is still quite high. Despite the fact that the optical counterparts of these γ-ray sources are still unknown, upon inspection, and after the test was carried out, it turned out that most of them have SEDs of the HBL type. A total of 80 cosmic rays are associated with this sample, to be compared with an expectation of 41.9 random associations. The probability of observing such an excess on randomized maps is 1.6×10^{-5} which translates into 0.055% (3.26σ) after compensation for trials. For the other catalogs considered, we observe similar but less significant excesses only for HBLs (see Fig. S2, S3, S4 in Supplemental Material at [URL will be inserted by publisher]). No cosmic ray excess is observed for sources not in spatial coincidence with IceCube neutrinos (see Fig. 2, dotted lines). The result of the likelihood ratio test described above is reported

TABLE I. γ - ν - CR correlation test results: local and global p-values obtained with respect to the γ-ray catalogs tested. The local p-value is the minimum p-value observed partitioning the γ-ray catalogs in F_γ (or FoM) and scanning in angular distance θ between neutrino spatially selected sources and CRs. The global p-value is the corresponding one penalized for the relative trials applied through the two dimensional scan. The p-value calculation is done using $10^6 - 10^7$ trials depending on the significance of the result. The results of the likelihood ratio test in Eq. (1) and the p-value of the outcome are listed in the last two columns.

γ-ray catalog	#	flux or FoM	θ (deg)	#γ-ray above flux (FoM)	#CRs observed	#CRs expected	local p-value (γ - ν - CR)	global p-value (γ - ν - CR)	$\log_{10}\Lambda$	Λ p-value
2FHL	360	0.25	10	146	83	45.8	3.6×10^{-5}	1.5×10^{-3}	3.57	2.0×10^{-3}
HBL	173	0.18	10	110	75	40.0	4.5×10^{-5}	1.4×10^{-3}	3.93	1.0×10^{-3}
+ uncl.	186	0.18	10	114	80	41.9	1.6×10^{-5}	5.5×10^{-4}	4.37	4.1×10^{-4}
non-HBL	174	0.35	10	56	37	19.8	1.2×10^{-2}	1.5×10^{-1}	0.63	2.4×10^{-1}
2WHSP	1681	2.51	17	38	75	30.6	2.7×10^{-4}	1.1×10^{-2}	2.68	9.8×10^{-3}
3LAC	1444	0.56	18	1000	231	200.3	1.9×10^{-2}	2.4×10^{-1}	0.40	3.1×10^{-1}
FSRQ	415	1.00	18	438	174	164.6	3.1×10^{-1}	8.9×10^{-1}	-0.99	8.3×10^{-1}
HBL	386	0.71	16	115	131	92.4	4.7×10^{-3}	9.3×10^{-2}	1.61	7.2×10^{-2}
other	645	1.00	3	285	19	11.8	3.3×10^{-2}	3.2×10^{-1}	0.19	4.0×10^{-1}

Note – For 2FHL (3LAC), the flux $F_\gamma\,(>50\,\mathrm{GeV})$ ($F_\gamma\,(>100\,\mathrm{MeV})$) is in units of $10^{-10}\,\mathrm{ph\,cm^{-2}\,s^{-1}}$ ($10^{-8}\,\mathrm{ph\,cm^{-2}\,s^{-1}}$). The 2WHSP catalog is scanned in the dimensionless quantity "figure of merit" (FoM) as introduced in the text and [45].

in Fig. S1 and Tab. I. With a p-value of 0.041% (3.35σ), the alternative model $\nu_\oplus$ (UHECRs correlate with sources in spatial coincidence with neutrinos) is favored providing an evidence of an association between HBLs and UHECRs.

Discussion.– Out of the 51 IceCube events, only 17 are associated with at least one γ-ray counterpart for our best p-value (2FHL HBLs + unclassified sample). This is one more than in [33] because here we do not exclude the Galactic plane; none of these is a track. All but one of the γ-ray sources associated with a neutrino have between one and seven UHECRs associated within 10°.

As mentioned above, we see 80 cosmic rays compared to an expectation of 41.9. If these numbers are compared to the total of 303 cosmic rays used in this study, $12.5^{+2.6}_{-2.2}$% of the entire cosmic ray flux could be interpreted as physically connected to extreme HBLs, leaving room for additional components. We note that this value is intriguingly close to the fraction of the IceCube signal explained by the same type of sources ($\sim 10-20\%$) [10, 33].

Among the selected sources, there are also relatively close-by, well-known, TeV emitters such as MKN 421 (also discussed in [46]), PKS 2005–489, and 1ES 1011+496. Given the redshifts of some of the sources (see Tab. S1 in Supplemental Material at [URL will be inserted by publisher]), the scenario proposed here might seem to be in some tension with the expected GZK suppression (and other CR-background interactions). However: 1. the mean energy loss distance for protons with $E \sim 50-60\times10^{18}\,\mathrm{eV}$ have been recently computed to be possibly up to $z \approx 0.2$ (e.g. [47]); 2. the majority of the HBLs do not have a distance determination (and therefore their redshift distribution is not very informative); 3. about half of the sources are expected to be spurious; 4. the intrinsic source power in UHECRs is unknown.

UHECRs propagating through space will contribute to the diffuse γ-ray emission via pion photoproduction on the CMB photons. Hence, the scenario proposed here has to be questioned also on these terms. Recent work [48] has discussed the contribution of HBLs to the Extragalactic Gamma Ray Background (EGRB) detected by *Fermi*. Given that the EGRB is dominated by HBLs [49, 50], there is little room to accommodate the inevitable diffuse contribution from γ-rays resulting from UHECR losses during propagation. Once blazar evolution is correctly taken into account as done in [48], however, the secondary γ-ray radiation expected from HBL blazars, which do not show cosmological evolution and are a small subset of the entire blazar population, is much lower than for other classes leaving these objects as viable sources of UHECRs. At the same time, the expected cosmogenic (GZK) neutrino flux would also be very low [51].

We stress that, although at first glance our results appear to have a p-value similar to that obtained by [37], as discussed in the Introduction and also noted by the authors, their best value applies to the UHECR randomization case, which is patently dominated by the presence of hot spots in the UHECR sky. This is not our case since we, on purpose, randomize the right ascensions of the neutrino events.

Conclusion.– We have provided evidence (p-value = 0.041%; 3.35σ) that a sub-class of blazars may be the counterpart of some high energy neutrinos and

UHECRs. These are extreme blazars, i.e. strong, very high energy γ-ray sources of the high energy peaked type. Due to the limited angular resolution of the IceCube neutrinos and the intrinsic magnetic bending of the UHECRs, one cannot determine at present which of the counterparts selected is indeed responsible for the multi-messenger emission. Larger samples of UHECRs, including new data and events with $E < 52 \times 10^{18}$ eV, and of neutrinos, would allow us to test further and with better statistics this first evidence but unfortunately these data are still proprietary. We therefore suggest the international collaborations to follow up on this or alternatively make their catalogs publicly available.

Acknowledgments.– We acknowledge useful discussions with Ralf Engel, Piera Ghia, and Thierry Lasserre. We thank the many teams, which have produced the data and catalogs used in this paper for making this work possible. ER is supported by the Heisenberg Program of the Deutsche Forschungsgemeinschaft (DFG RE 2262/4-1), SC by the cluster of excellence "Origin and Structure of the Universe" of the Deutsche Forschungsgemeinschaft.

[1] C. M. Urry and P. Padovani, Publ. Astron. Soc. Pac. **107**, 803 (1995), arXiv:astro-ph/9506063 [astro-ph].
[2] Blazars are subdivided in two main sub-classes, namely flat-spectrum radio quasars (FSRQ) and BL Lacertae objects (BL Lacs), with the former displaying strong, broad emission lines and the latter instead being characterized by optical spectra showing at most weak emission lines, sometimes exhibiting absorption features, and in many cases being completely featureless.
[3] P. Padovani and P. Giommi, Astrophys. J. **444**, 567 (1995), arXiv:astro-ph/9412073 [astro-ph].
[4] K. Mannheim, Astropart. Phys. **3**, 295 (1995).
[5] F. Halzen and E. Zas, Astrophys. J. **488**, 669 (1997), arXiv:astro-ph/9702193 [astro-ph].
[6] A. Muecke, R. J. Protheroe, R. Engel, J. P. Rachen, and T. Stanev, Astropart. Phys. **18**, 593 (2003), arXiv:astro-ph/0206164 [astro-ph].
[7] M. D. Kistler, T. Stanev, and H. Yüksel, Phys. Rev. **D90**, 123006 (2014), arXiv:1301.1703 [astro-ph.HE].
[8] K. Murase, Y. Inoue, and C. D. Dermer, Phys. Rev. **D90**, 023007 (2014), arXiv:1403.4089 [astro-ph.HE].
[9] F. Tavecchio and G. Ghisellini, Mon. Not. Roy. Astron. Soc. **451**, 1502 (2015), arXiv:1411.2783 [astro-ph.HE].
[10] P. Padovani, M. Petropoulou, P. Giommi, and E. Resconi, Mon. Not. Roy. Astron. Soc. **452**, 1877 (2015), arXiv:1506.09135 [astro-ph.HE].
[11] M. D. Kistler and R. Laha, ArXiv e-prints (2016), arXiv:1605.08781 [astro-ph.HE].
[12] T. K. Gaisser, R. Engel, and E. Resconi, *Cosmic Rays and Particle Physics* (Cambridge University Press, 2016).
[13] J. Abraham *et al.* (Pierre Auger), Nucl. Instrum. Meth. **A523**, 50 (2004).
[14] A. Aab *et al.* (Pierre Auger), Nucl. Instrum. Meth. **A798**, 172 (2015), arXiv:1502.01323 [astro-ph.IM].
[15] T. Abu-Zayyad *et al.* (Telescope Array), Nucl. Instrum. Meth. **A689**, 87 (2013), arXiv:1201.4964 [astro-ph.IM].
[16] A. Aab *et al.* (Pierre Auger), Astrophys. J. **804**, 15 (2015), arXiv:1411.6111 [astro-ph.HE].
[17] T. Abu-Zayyad *et al.* (Telescope Array), Astrophys. J. **777**, 88 (2013), arXiv:1306.5808 [astro-ph.HE].
[18] R. U. Abbasi *et al.* (Telescope Array), Astrophys. J. **790**, L21 (2014), arXiv:1404.5890 [astro-ph.HE].
[19] M. G. Aartsen *et al.* (IceCube), Science **342**, 1242856 (2013), arXiv:1311.5238 [astro-ph.HE].
[20] M. G. Aartsen *et al.* (IceCube), Phys. Rev. Lett. **113**, 101101 (2014), arXiv:1405.5303 [astro-ph.HE].
[21] M. G. Aartsen *et al.* (IceCube), ArXiv e-prints (2015), arXiv:1510.05222 [astro-ph.HE].
[22] Shower-like events are one of the topologies for neutrino observatories. Showers have a good energy resolution but reduced angular resolution ($\sim 10^\circ$). The other topology are track-like events induced by muons, that have much better angular resolution ($< 1^\circ$), in which not all the energy is deposited in the detector.
[23] M. G. Aartsen *et al.* (IceCube), ArXiv e-prints (2015), arXiv:1510.05223 [astro-ph.HE].
[24] M. G. Aartsen *et al.* (IceCube), arXiv:1607.08006 [astro-ph.HE].
[25] B. Khiali and E. M. de Gouveia Dal Pino, Monthly Notices of the Royal Astronomical Society **455**, 838 (2016), arXiv:1506.01063 [astro-ph.HE].
[26] R. Moharana, R. J. G. Britto, and S. Razzaque, ArXiv e-prints (2016), arXiv:1602.03694 [astro-ph.HE].
[27] K. Murase, D. Guetta, and M. Ahlers, Physical Review Letters **116**, 071101 (2016), arXiv:1509.00805 [astro-ph.HE].
[28] I. Tamborra and S. Ando, Phys. Rev. D **93**, 053010 (2016), arXiv:1512.01559 [astro-ph.HE].
[29] N. Senno, K. Murase, and P. Mészáros, Phys. Rev. D **93**, 083003 (2016), arXiv:1512.08513 [astro-ph.HE].
[30] X.-Y. Wang and R.-Y. Liu, Phys. Rev. D **93**, 083005 (2016), arXiv:1512.08596 [astro-ph.HE].
[31] V. N. Zirakashvili and V. S. Ptuskin, Astroparticle Physics **78**, 28 (2016), arXiv:1510.08387 [astro-ph.HE].
[32] A. Neronov and D. Semikoz, Phys. Rev. D **93**, 123002 (2016), arXiv:1603.06733 [astro-ph.HE].
[33] P. Padovani, E. Resconi, P. Giommi, B. Arsioli, and Y. L. Chang, Mon. Not. Roy. Astron. Soc. **457**, 3582 (2016), arXiv:1601.06550 [astro-ph.HE].
[34] M. Ackermann *et al.* (Fermi-LAT), Astrophys. J. Suppl. **222**, 5 (2016), arXiv:1508.04449 [astro-ph.HE].
[35] M. G. Aartsen *et al.* (IceCube), Phys. Rev. Lett. **115**, 081102 (2015), arXiv:1507.04005 [astro-ph.HE].
[36] S. Schoenen and L. Raedel (IceCube), The Astronomer's Telegram **7856** (2015).
[37] M. G. Aartsen *et al.* (IceCube, Pierre Auger, Telescope Array), JCAP **1601**, 037 (2016), arXiv:1511.09408 [astro-ph.HE].
[38] M. Petropoulou, S. Dimitrakoudis, P. Padovani, A. Mastichiadis, and E. Resconi, Mon. Not. Roy. Astron. Soc. **448**, 2412 (2015), arXiv:1501.07115 [astro-ph.HE].
[39] Y.-L. Chang, B. Arsioli, P. Giommi, and P. Padovani, Astron. Astrophys., submitted (2016).
[40] M. Ackermann *et al.* (Fermi-LAT), Astrophys. J. **810**, 14 (2015), arXiv:1501.06054 [astro-ph.HE].
[41] The determination of ν_S, which is required to classify sources as HBLs, requires the availability of multi-

frequency data and is also affected by variability, a defining feature of blazars. The HBL - non-HBL distinction is therefore not sharp by definition.
[42] K. Greisen, Phys. Rev. Lett. **16**, 748 (1966).
[43] G. T. Zatsepin and V. A. Kuzmin, JETP Lett. **4**, 78 (1966), [Pisma Zh. Eksp. Teor. Fiz.4,114(1966)].
[44] The FoM is defined as the ratio between the synchrotron peak flux of a source and that of the faintest blazar in the WHSP sample already detected in the TeV band.
[45] B. Arsioli, B. Fraga, P. Giommi, P. Padovani, and P. M. Marrese, Astron. Astrophys. **579**, A34 (2015), arXiv:1504.02801 [astro-ph.HE].
[46] K. Fang, T. Fujii, T. Linden, and A. V. Olinto, Astrophys. J. **794**, 126 (2014), arXiv:1404.6237 [astro-ph.HE].
[47] R. Ruffini, G. V. Vereshchagin, and S. S. Xue, Astrophys. Space Sci. **361**, 82 (2016), arXiv:1503.07749 [astro-ph.HE].
[48] E. Gavish and D. Eichler, Astrophys. J. **822**, 56 (2016), arXiv:1603.04074 [astro-ph.HE].
[49] P. Giommi and P. Padovani, Mon. Not. Roy. Astron. Soc. **450**, 2404 (2015), arXiv:1504.01978 [astro-ph.HE].
[50] M. Ajello *et al.*, Astrophys. J. **800**, L27 (2015), arXiv:1501.05301 [astro-ph.HE].
[51] A. M. Taylor, M. Ahlers, and D. Hooper, Phys. Rev. **D92**, 063011 (2015), arXiv:1505.06090 [astro-ph.HE].

SUPPLEMENTARY MATERIAL

Results of the likelihood ratio test Λ for the 2FHL catalog.– The outcome of the likelihood ratio test Λ (Eq. (1)) is shown in Fig. S3 for the 2FHL catalog. With a p-value of 0.041% (3.35σ), the alternative model $\nu_{\oplus}$ (UHECRs correlate with sources in spatial coincidence with neutrinos) is favored providing an evidence of an association between HBLs and UHECRs.

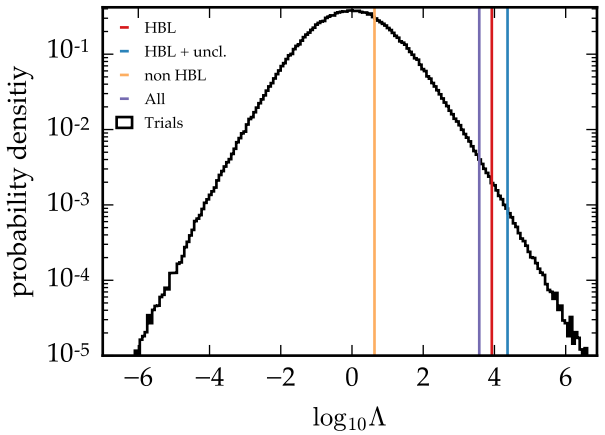

FIG. S3. Result of the likelihood ratio test Λ described in Eq. (1) for the 2FHL catalog. Large values of Λ indicate preference of a connection between γ-rays and UHECRs in coincidence with neutrinos. Vertical lines show the outcome of the test for a partition of the catalog with respect to random trials (black histogram).

Results for the 2WHSP and 3LAC catalogs.– Table I lists the results for all catalogs used in this work. As highlighted in the discussion section, a strong correlation for HBL type objects in the 2FHL catalog is found. The 2WHSP catalog [45] consists only of blazars of the HBL type excluding the Galactic Plane ($|b_{\rm II}| \geq 10°$). The best (lowest) p-value is found for a "figure of merit" FoM $\geq$ 2.51 and UHECR angular distance $\theta = 17°$. 75 UHECR events are observed above an expectation of 30.6. The local p-value at this point is 2.7×10^{-4} and increases to 1.1% (2.29σ) after trial correction. The scan in FoM and θ is shown in Fig. S4. The 3LAC catalog [40] includes HBLs, FSRQ, and other types of sources. As listed in Tab. I, the most significant result is again obtained for objects of the HBL type, consistent with the result of the 2FHL catalog. The scan in F_γ and θ is shown in Fig. S5. The most significant correlation is observed for HBL objects with flux $F_\gamma\,(>100\,\mathrm{MeV}) \geq 0.71 \times 10^{-8}\ \mathrm{ph\,cm^{-2}\,s^{-1}}$ and $\theta = 17°$. 131 UHECR events are observed above an expectation of 92.4. The local p-value of this observation yields 4.7×10^{-3}. After trial correction this increases to

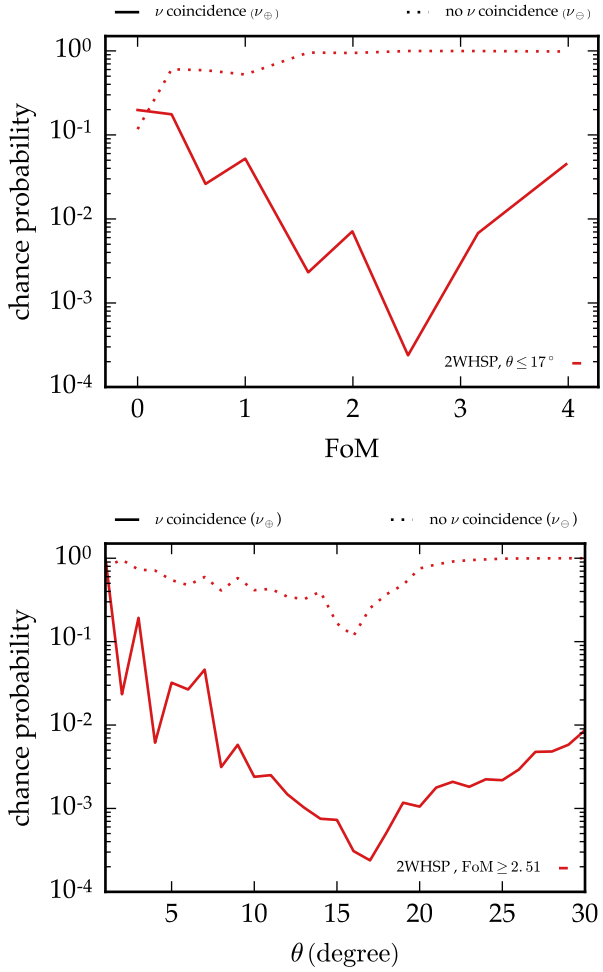

FIG. S4. Result of the statistical test for the 2WHSP catalog scanning over "figure of merit" (FoM, top) and UHECR angular distance θ (bottom). Solid lines indicate the outcome for UHECRs correlating with γ-ray objects in coincidence with neutrinos ($\nu_\oplus$), dotted lines with no coincidence with neutrinos ($\nu_\ominus$).

9.3%. The other types of objects in the catalog (FSRQ and others) show a non significant correlation with trial corrected p-values of 89% and 32%, respectively. The outcome of the likelihood ratio test Λ (Eq. (1)) is shown in Fig. S6 for the 2WHSP (left) and 3LAC catalog (right). The test for the 2WHSP indicates a result in favor of positive neutrino correlation $\nu_\oplus$ at a p-value 0.98% (2.3σ). For 3LAC, the result is 7.2%, again more significant for HBLs than for the remaining subsets of the catalog.

UHECRs in correlation with 2FHL objects.– The most significant result was seen for neutrinos and UHECRs correlating with 2FHL objects of the HBL type and unclassified. Tab. S2 lists the clusters of neutrinos correlating with 2FHL objects and UHECRs. Fur-

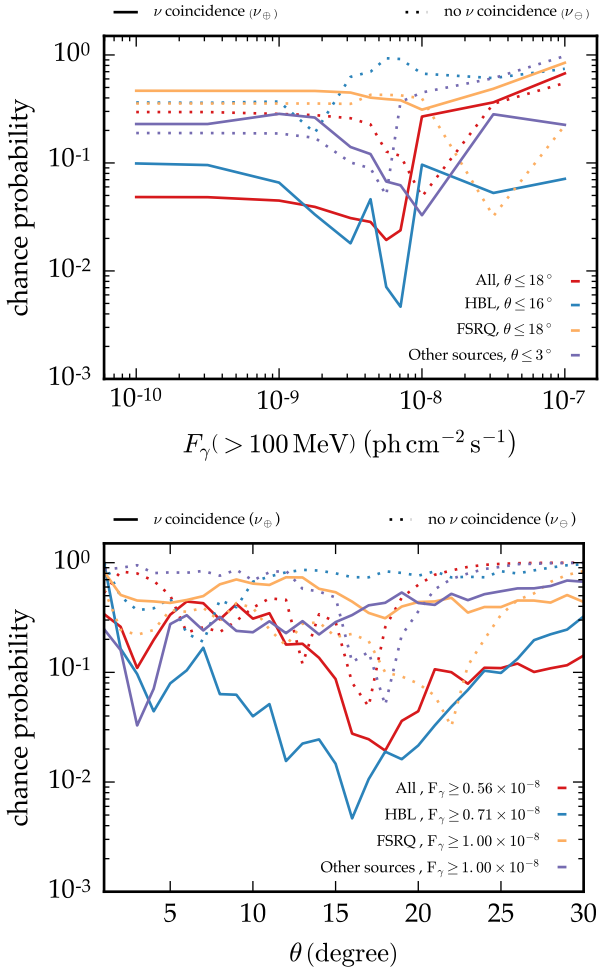
ν coincidence ($\nu_\oplus$)
no ν coincidence ($\nu_\ominus$)
chance probability
All, $\theta \leq 18^\circ$
HBL, $\theta \leq 16^\circ$
FSRQ, $\theta \leq 18^\circ$
Other sources, $\theta \leq 3^\circ$
$F_\gamma(>100\,\mathrm{MeV})\,(\mathrm{ph\,cm^{-2}\,s^{-1}})$
ν coincidence ($\nu_\oplus$)
no ν coincidence ($\nu_\ominus$)
chance probability
All , $F_\gamma \geq 0.56 \times 10^{-8}$
HBL , $F_\gamma \geq 0.71 \times 10^{-8}$
FSRQ , $F_\gamma \geq 1.00 \times 10^{-8}$
Other sources , $F_\gamma \geq 1.00 \times 10^{-8}$
θ (degree)

FIG. S5. Result of the statistical test for partitions of the 3LAC catalog over flux $F_\gamma\,(>100\,\mathrm{MeV})$ (left) and UHECR angular distance θ (right). Solid lines indicate the outcome for UHECRs correlating with γ-ray objects in coincidence with neutrinos ($\nu_\oplus$), dotted lines with no coincidence with neutrinos ($\nu_\ominus$)

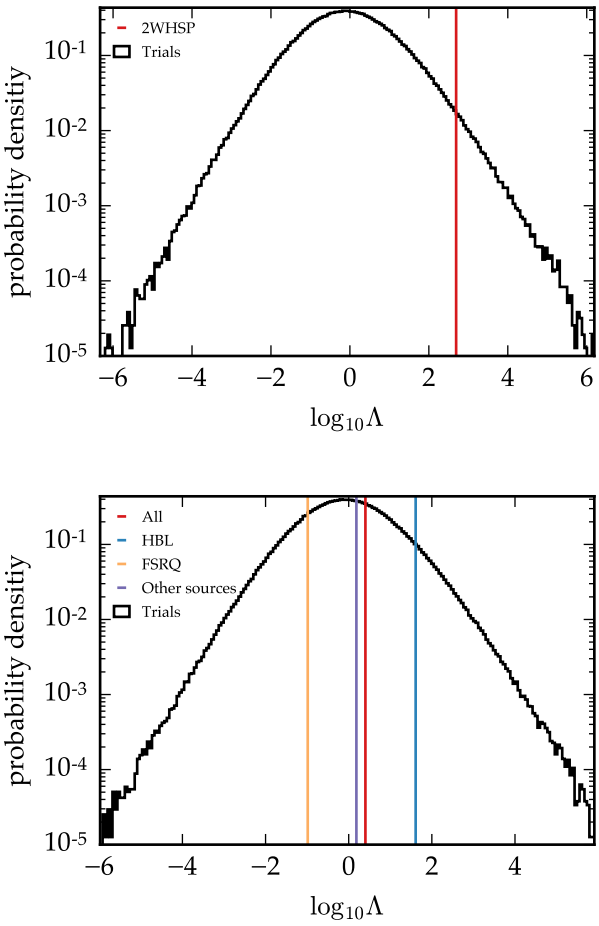

FIG. S6. Result of the likelihood ratio test Λ defined in Eq. (1) for the 2WHSP (left) and partitions of the 3LAC catalog (right). Vertical lines indicate the outcome of the test using a catalog with respect to the distribution of random trials (black histogram) as listed in Tab. I.

thermore, information about the events and objects is listed. Namely: the neutrino energy and angular resolution, the redshift of the object (if known), the position of the UHECR event, plus its energy and distance from the 2FHL object. We include also the redshift (z) distribution for the 2FHL objects type HBL and unclassified Fig. S7.

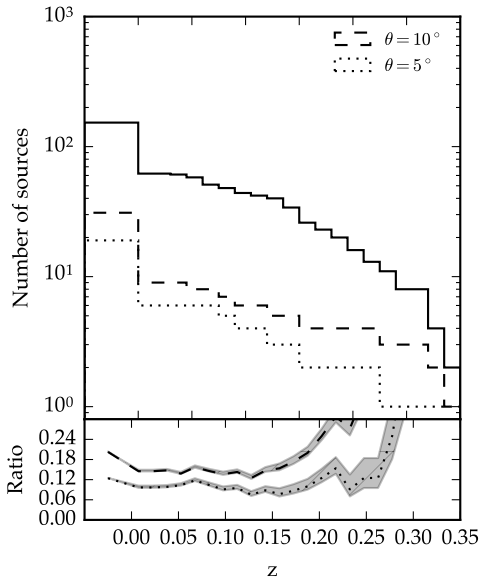

FIG. S7. Top: redshift (z) distribution for the 2FHL objects type HBL and unclassified (continuous line), at an angular distance $<10^o$ from the UHECRs (dashed line), and at an angular distance $<5^o$ from the UHECRs (dotted line). The sources without a measured z are counted in the bin below zero. Bottom: ratio between the two lower lines and the upper line in the top plot.

TABLE S2: IceCube neutrinos, 2FHL objects (type HBL and unclassified) and Auger/TA UHECRs selected in correspondence with the minimum p-value obtained ($F_\gamma\,(>50\,\mathrm{GeV}) \geq 1.8\times10^{-11}\,\mathrm{ph\,cm^{-2}\,s^{-1}}$ and $\theta \leq 10^\circ$). We report for each neutrino the ID number, the energy and the median angular uncertainty (median$(\theta)_{\mathrm{IC}}$) as quoted by IceCube; for the γ-ray objects the *Fermi* source name and common name, and if known, the redshift; for the UHECRs the year of detection, the coordinates, the dataset, the energy and angular distance from the 2FHL object.

High Energy Neutrino			γ-ray Source			Ultra High Energy Cosmic Ray					
ID	Energy (TeV)	median$(\theta)_{\mathrm{IC}}$ (deg)	2FHL name	Common name	z	Year	RA	Dec	Dataset	Energy (EeV)	θ (deg)
9	63.2	16.5	J0915.9+2931	B2 0912+29	0.19	2013	138.6	26.1	Auger	62.1	3.4
						2008	140.0	28.7	TA	59.2	1.0
						2010	129.0	29.1	TA	60.5	8.5
			J0910.4+3327	Ton 1015	0.35	2013	138.6	26.1	Auger	62.1	7.4
						2008	140.0	28.7	TA	59.2	5.1
						2010	145.0	40.7	TA	92.2	9.1
						2010	137.0	41.5	TA	68.9	8.1
						2010	129.0	29.1	TA	60.5	8.3
			J1104.4+3812	MKN 421	0.03	2011	163.7	28.9	TA	62.3	9.5
						2011	157.0	38.8	TA	72.9	7.3
						2012	160.0	35.6	TA	57.4	5.7
			J1015.0+4926	1ES 1011+496	0.20	2008	152.4	45.8	TA	79.3	3.7
						2010	139.0	49.6	TA	63.7	9.5
						2013	165.0	52.4	TA	62.5	7.8
11	88.4	16.7	J1027.0–1749	1RXS J102658.5–174905	0.65	2009	147.2	−18.3	Auger	64.1	9.1
						2011	150.0	−10.3	Auger	100.0	9.9
						2011	149.0	−13.0	Auger	57.2	9.0
						2013	154.0	−15.8	Auger	53.9	3.1
			J0952.9–0841	1RXS J095303.4–084003	–	2006	142.3	−13.1	Auger	54.0	7.3
						2009	147.0	−18.3	Auger	64.1	9.6
						2011	150.0	−10.3	Auger	100.0	2.4
						2011	149.0	−13.0	Auger	57.2	4.3
						2013	154.0	−15.8	Auger	53.9	9.3
12	104	9.8	J2009.4–4849	PKS 2005–489	0.07	2006	305.6	−46.3	Auger	60.0	3.3
						2007	315.0	−53.8	Auger	72.7	9.4
						2008	306.0	−55.1	Auger	55.1	6.8
			J1959.6–4725	SUMSS J195945–472519	–	2006	305.6	−46.3	Auger	60.1	4.0
						2008	306.0	−55.1	Auger	55.1	8.7
						2013	308.0	−39.5	Auger	67.3	9.9
			J1936.9–4721	PMN J1936–4719	0.26	2006	305.6	−46.3	Auger	60.1	7.8
						2013	287.0	−55.0	Auger	52.9	9.0
14	1041	13.2	J1713.9–2027	1RXS J171405.2–202747	–	2008	252.7	−22.7	Auger	64.2	5.9
			J1823.6-3454	NVSS J182338–345412	–	2013	284.5	−37.6	Auger	54.4	7.4
						2009	286.0	−37.8	Auger	61.0	8.8
						2009	276.0	−33.4	Auger	65.8	1.5
						2011	284.0	−28.6	Auger	80.9	9.2
			J1829.0–2417	1RXS J182853.8–241746	–	2010	284.7	−28.2	Auger	65.2	7.6
						2009	276.0	−33.4	Auger	65.8	9.1
						2011	284.0	−28.6	Auger	80.9	7.1
			J1741.2–4021		–	2010	258.1	−44.9	Auger	72.9	7.0
						2012	260.0	−32.7	Auger	61.8	8.9
17	200	11.6	J1555.7+1111	PG 1553+113	0.44	2007	245.8	8.5	Auger	54.9	7.3
						2011	239.0	3.9	Auger	60.3	7.3
19	71.5	9.7	J0543.9–5533	1RXS J054357.3–553206	0.27	2010	80.2	−64.1	Auger	54.3	9.0
						2013	92.1	−64.1	Auger	65.4	9.1
						2013	91.4	−60.6	Auger	72.5	5.8
20	1141	10.7	J0352.7–6831	PKS 0352–686	0.08	2012	37.0	−75.8	Auger	58.7	9.6
						2014	45.2	−65.8	Auger	63.6	5.7
						2010	80.2	−64.1	Auger	54.3	9.8
						2013	56.6	−67.8	Auger	70.7	0.9
						2013	64.7	−70.1	Auger	68.8	2.8

TABLE S2: continued

High Energy Neutrino			γ-ray Source			Ultra High Energy Cosmic Ray					
ID	Energy (TeV)	median$(\theta)_{\rm IC}$ (deg)	2FHL name	Common name	z	Year	RA	Dec	Dataset	Energy (EeV)	θ (deg)
						2014	72.8	−73.5	Auger	60.0	6.8
22	220	12.1	J1958.3–3011	1RXS J195815.6–30111	0.12	2011	295.1	−27.6	Auger	54.8	4.7
						2008	304.0	−26.2	Auger	52.6	5.8
						2011	305.0	−34.5	Auger	67.4	6.6
			J1917.7–1921	1H1914–194	0.14	2010	284.7	−28.2	Auger	65.2	9.8
						2011	295.0	−27.6	Auger	54.8	9.8
						2009	294.0	−20.5	Auger	59.5	4.9
			J1921.9–1607	PMNJ1921–1607	–	2009	294.5	−20.5	Auger	59.5	5.8
26	210	11.8	J0905.7+1359	MG1 J090534+1358	1.07	2011	132.8	12.9	Auger	55.9	3.7
						2007	137.0	6.2	Auger	53.6	7.9
						2009	129.0	15.2	Auger	52.2	6.9
			J0915.9+2931	B2 0912+29	0.19	2013	138.6	26.1	Auger	62.1	3.4
						2008	140.0	28.7	TA	59.2	1.0
						2010	129.0	29.1	TA	60.5	8.5
27	60.2	6.6	J0816.3–1311	PMN J0816–1311	–	2010	131.9	−15.5	Auger	76.1	7.9
						2013	123.0	−6.2	Auger	85.3	7.0
33	385	13.5	J1933.3+0725	1RXS J193320.3+072616	–	2008	287.7	1.5	Auger	118.0	8.2
						2013	299.0	8.7	Auger	54.6	5.4
						2011	288.0	0.3	TA	136.0	8.8
			J1931.1+0937	RX J1931.1+0937	–	2008	287.7	1.5	Auger	118.3	9.6
						2013	299.0	8.7	Auger	54.6	5.9
			J1942.8+1033	1RXS J194246.3+103339	–	2006	299.0	19.4	Auger	82.0	9.4
						2013	299.0	8.7	Auger	54.6	3.5
35	2004	15.9	J1328.6–4728	1WGA J1328.6–4727	–	2005	199.1	−48.5	Auger	52.1	2.3
						2006	201.0	−55.3	Auger	69.5	7.8
						2006	201.0	−45.3	Auger	59.5	2.4
						2007	200.0	−43.4	Auger	60.0	4.3
						2008	202.0	−54.9	Auger	53.4	7.4
			J1304.5–4353	1RXS 130421.2–435308	–	2004	199.7	−34.8	Auger	84.7	9.4
						2005	199.0	−48.5	Auger	52.1	5.1
						2006	201.0	−45.3	Auger	59.5	3.7
						2007	200.0	−43.4	Auger	60.0	3.0
						2007	193.0	−35.3	Auger	60.7	9.0
						2009	194.0	−36.4	Auger	72.5	7.7
			J1307.6–4259	1RXS 130737.8–425940	–	2004	199.7	−34.8	Auger	84.7	8.4
						2005	199.0	−48.5	Auger	52.1	5.8
						2006	201.0	−45.3	Auger	59.5	3.7
						2007	200.0	−43.4	Auger	60.0	2.4
						2007	193.0	−35.3	Auger	60.7	8.4
						2009	194.0	−36.4	Auger	72.5	7.0
						2013	201.0	−34.6	Auger	62.7	9.0
			J1353.5–6640	1RXS J135341.1–664002	–	2007	195.5	−63.4	Auger	61.9	6.3
						2008	196.0	−69.7	Auger	71.1	5.5
						2013	199.0	−63.9	Auger	53.2	4.9
						2004	208.0	−60.1	Auger	58.6	6.6
						2008	187.0	−63.5	Auger	65.3	9.3
						2010	216.0	−66.5	Auger	60.3	3.1
						2010	219.0	−70.8	Auger	89.1	5.6
			J1507.4–6213		–	2013	240.3	−68.9	Auger	61.5	8.7
						2004	208.0	−60.1	Auger	58.6	9.3
						2007	220.0	−53.9	Auger	61.5	9.2
						2010	216.0	−66.5	Auger	60.3	6.3
						2010	219.0	−70.8	Auger	89.1	9.2
						2010	232.0	−56.6	Auger	54.9	6.2
39	101.3	14.2	J0649.6–3139	1RXSJ064933.8–31391	–	2007	105.9	−22.8	Auger	60.8	9.3
			J0622.4–2604	PMNJ0622–2605	–	2007	105.9	−22.8	Auger	60.8	9.9
			J0631.0–2406	1RXSJ063059.7–240636	–	2007	105.9	−22.8	Auger	60.8	7.6
			J0639.9–1252		–	–	–	–	–	–	–
41	87.6	11.1	J0416.9+0105	1ES 0414+009	0.29	2008	67.7	4.0	Auger	52.0	4.5

TABLE S2: continued

High Energy Neutrino			γ-ray Source			Ultra High Energy Cosmic Ray					
ID	Energy (TeV)	median$(\theta)_{\rm IC}$ (deg)	2FHL name	Common name	z	Year	RA	Dec	Dataset	Energy (EeV)	θ (deg)
						2012	56.4	−3.2	Auger	53.3	9.0
46	158	7.6	J1027.0–1749	1RXS J102658.5–174905	0.65	2009	147.2	−18.2	Auger	64.1	9.1
						2011	150.0	−10.3	Auger	100.0	9.9
						2011	149.0	−13.0	Auger	57.2	9.0
						2013	154.0	−15.8	Auger	53.9	3.1
48	104.7	8.1	J1440.7–3847	1RXS J144037.4–38465	–	2004	224.7	−44.0	Auger	58.2	6.2
						2008	221.0	−42.8	Auger	73.1	4.0
						2011	219.0	−41.9	Auger	58.8	3.2
51	66.2	6.5	J0540.5+5822	GB6 J0540+5823	–	2009	99.2	62.7	TA	80.7	8.1
						2010	78.8	61.4	TA	61.2	4.4
						2011	82.5	57.7	TA	74.7	1.6